Fatigue Behaviour of Welded Joints Treated by High Frequency Hammer Peening: Part I , Experimental Study

Guenhael Le Quilliec, Henri-Paul Lieurade, Marc Bousseau, Monssef Drissi-Habti, Geneviève Inglebert, Pascal Macquet, Laurent Jubin

Fatigue Behaviour of Welded Joints Treated by High Frequency Hammer Peening: Part I, Experimental Study

Conference Paper · July 2011

CITATIONS
3

READS
133

7 authors, including:

Guenhael Le Quilliec
University of Tours
41 PUBLICATIONS **43** CITATIONS

SEE PROFILE

INTERNATIONAL INSTITUTE OF WELDING
A world of joining experience

French Delegation

IIW document XIII-2394-11

Fatigue Behaviour of Welded Joints Treated by High Frequency Hammer Peening: Part I, Experimental Study

G. Le Quilliec[1,2,3], H.-P. Lieurade[1], M. Bousseau[4], M. Drissi-Habti[2], G. Inglebert[3], P. Macquet[1], L. Jubin[1]

[1]CETIM, centres of Senlis and Nantes, France.
[2]IFSTTAR, centre of Nantes, France.
[3]LISMMA, Supméca of Paris, France.
[4]CESMAN - DCNS Research, Indret, France.
Contact: guenhael.lequilliec@yahoo.fr

Abstract: High frequency hammer peening is a recent improvement method which is probably one of the most effective for treating welded assemblies. A number of experimental results relating to this process are presented in this article. These results lead to better understand the mechanisms of the process, to outline the influence of the operating parameters and to confirm the role played by the initial quality of the welds. In the long run, the aim of this study is to propose an industrially applicable approach for the fatigue design of welded assemblies treated by high frequency hammer peening. The numerical study carried out in parallel is presented in the IIW document: XIII-2395-11.

Keywords: high frequency hammer peening, hammering, fatigue testing, steel welded assemblies, experimental investigation, post-weld treatment.

1 Introduction

In comparison with the base and filler materials used, welded structures have relatively low fatigue strength. This can be explained by the number of cycles required for a micro-crack to initiate. The initiation stage is often predominant in the fatigue life of metallic materials. It becomes very weak in the specific case of welded assemblies. This is mainly caused by the usual presence of residual tensile stresses, high stress raisers and an often poor surface roughness at the weld toe. It is therefore essential to have a design that takes into account the specific features in the case of exposure to cyclic loading. In addition, the precise study of the loading that will be undergone by the welded assembly will enable better design of the welded connection and make it possible to justify whether or not post treatments should be applied. These treatments will make possible to save weight. This gain will be all the more significant since the stresses will be limited and ultimate tensile strength will be high.

One of the most recent (and probably one of the most efficient) improvement methods is high frequency hammer peening or HFH [Le Quilliec et al., 2009]. With respect to conventional hammer peening, HFH stands out thanks to its improved simplicity and user comfort. Applying this treatment has been shown to be very competitive making the most of the advantages provided by certain materials in the field of welding and more particularly high strength steels. However, there is a certain number of technical difficulties that must be overcome to apply HFH whether for new or old structures. Using the various results available for this process is uneasy for the fatigue design of an HFH treated welded assembly for a given configuration and treatment parameters. Moreover, premature failures are often observed and the cause of these early failures is not clearly identified.

The work presented in this article falls within the framework of a project which should in the long run propose an industrially applicable approach with the aim of increasing the guaranteed fatigue life of new structures and to extend the one of existing structures. The experimental study of the HFH carried out on a cruciform welded assembly will be presented in the body of the text. The numerical study carried out in parallel is presented in the document IIW: XIII-2395-11.

2 Analysis of the as-welded state of the selected welded assembly

2.1 Configuration of the welded assembly

Cruciform non-carrying-fillet welded joints are one of the most common structural details of welded structures as well as the most susceptible to fatigue phenomenon. This assembly configuration was therefore selected for the HFH study in S355K2 grade rolled structural steel, a grade that is just as commonly used (as per standard NF EN 10025-2, 2005).

According to this standard, the yield strength of the base metal at ambient temperature in the rolling direction must be at least 355 MPa for an ultimate tensile strength ranging between 470 and 630 MPa. The thickness of the sheet used for the main plate and the attachments is 15 mm (Figure 1). The weld test coupons manufactured are each 1 m long and 250 mm wide with a total height at the attachments of 115 mm. The edges were not prepared in any special way prior to one-pass welding (cross passes) with a flux-cored type filler metal which has a similar grade (T42 4 MC 2H5) to that of the base metal. Finally, all the assemblies were performed with the automatic MAG process which makes it possible to ensure a good quality as well as proper repeatability of the operation on each run. The welding operation was carried out in flat position which results in run profiles that have a higher quality with regard to fatigue strength.

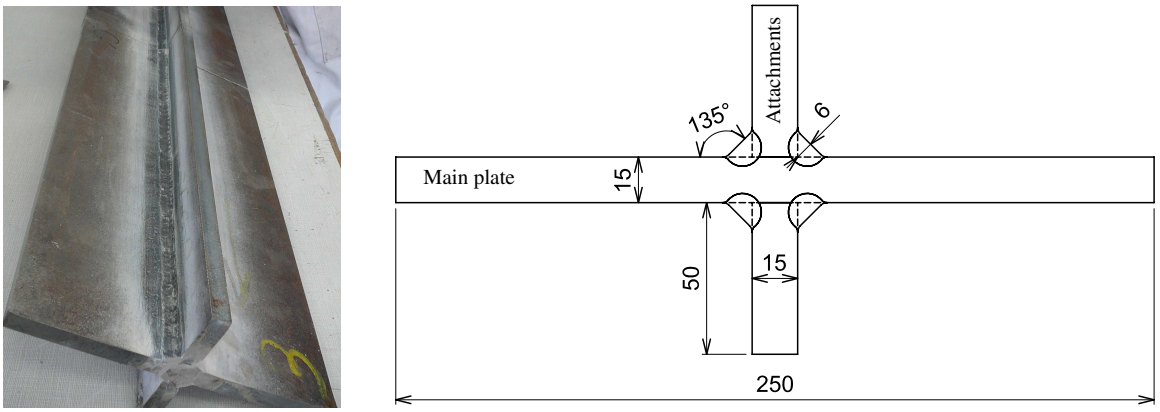

Figure 1: Selected configuration of the cruciform joints.

2.2 Geometrical measurements of the as-welded weld run

The detailed geometry of welded assemblies was analysed using a laser triangulation portable dimensional measuring device.

The overall geometry of a welded assembly is quickly characterized and inspected with this technology. Figure 2 illustrates the position of the system during measurement.

The statistical analysis carried out after measurements on all the welded assemblies is presented in table 1 (a detailed definition of the various parameters is given in figure 3). In accordance with the even appearance of these assemblies, the standard deviations obtained reveal a low dispersion of the values. The mean toe radius, given the position of the weld is greater than standard quality, of approximately 1.5 mm in MAG welding. The depth of the undercut measured, which is of approximately the same magnitude of resolution of the measuring device (0.05 mm), is insignificant.

Figure 2: Laser triangulation dimensional analysis (WISC process).

	Attachment orientation a [°]	**Main plate leg** b [mm]	**Attachment leg** c [mm]	**Throat** d [mm]	**Attachment undercut** e [mm]	**Main plate undercut** f [mm]
Average	90.13	9.23	8.04	5.30	0.04	0.05
Std deviation	0.44	0.50	0.62	0.24	0.05	0.05
Minimum	87.00	7.30	5.36	3.58	0.00	0.00
Maximum	93.90	12.12	13.42	6.96	0.98	1.00

	Attachment toe angle g [°]	**Main plate toe angle** h [°]	**Convexity** i [mm]	**Attachment toe radius** r_1 [mm]	**Main plate toe radius** r_2 [mm]
Average	143.10	148.61	-0.87	3.50	4.40
Std deviation	4.11	3.31	0.25	1.60	2.29
Minimum	121.20	116.80	-4.20	0.00	0.00
Maximum	161.40	167.50	0.90	11.36	13.74

Tab. 1: Results of the geometrical analysis by WISC process on the as-welded assemblies.

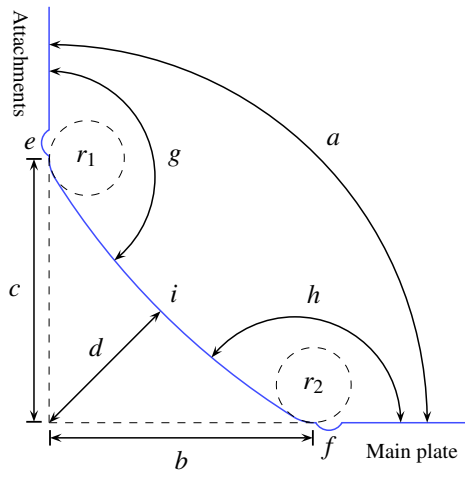

Figure 3: Definitions of the various parameters characterizing the geometry of the weld run.

2.3 Monotonic tensile tests

Standard NF EN 10025-2 [2005] only provides the ranges of the main mechanical characteristics that must be fulfilled for the selected S355K2 grade steel. Consequently, monotonic tensile tests were performed on the base metal used as well as on weld metal specimens. Welded samples has been obtained from a butt-welded assembly which has been especially carried out with the same base and filler materials as for the cruciform assembly. As opposed to the cruciform assemblies, the single-V butt-welded assemblies allow samples of traditional sized tensile specimens to be taken. However, the thermal cycle as well as the dilution phenomena between the items to be assembled and the filler product vary depending on the configuration. The mechanical behaviour obtained in the weld zone of the butt-welded assembly consequently differs from that of the cruciform assembly. However it is worth noting that this validation "practice" is common in the welding field.

According to the engineering tensile curves presented in figure 4, the Young's modulus measured is approximately 205 GPa for the base metal and 210 GPa for the weld metal. The offset yield strength at 0.2 % of the strain ($R_{p0.2}$) and the ultimate tensile strength are respectively 386 and 541 MPa for the base metal whereas those of the weld metal are 407 and 512 MPa. The presence of a significant Lüders plateau should also be noted for the weld metal.

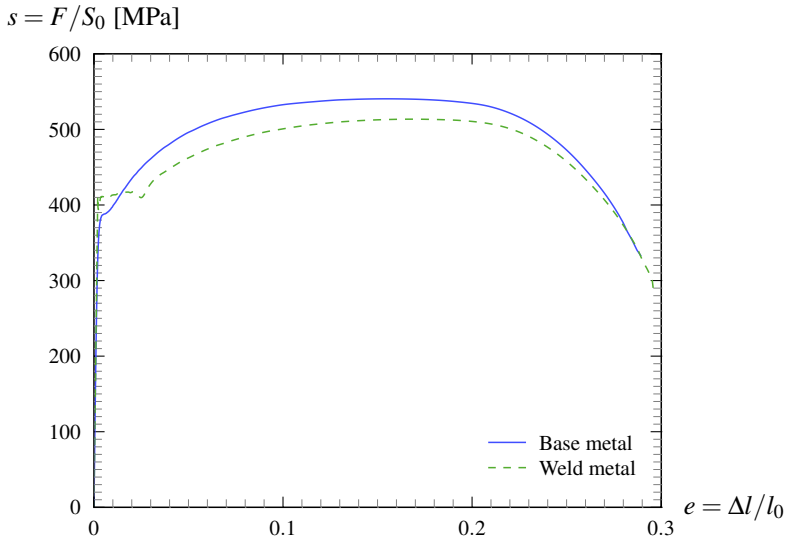

Figure 4: Engineering tensile curves of the base metal and the weld metal.

2.4 Low-cycle fatigue tests

In addition to the monotonic tensile tests, low-cycle fatigue tests were carried out on the base metal. The results obtained will be used during high cycle fatigue design of the welded assemblies. In addition, the cyclic tensile tests performed make it possible to characterize the type of hardening, mainly kinematic in this case as shown in figure 5.

All the cyclic properties estimated from the experimental tests are given in table 2. The values estimated by the Universal Material Law (UML), proposed by Bäumel and Seeger [1990], and the medians method, proposed by Meggiolaro and Castro [2004], are also given. These two methods are based on statistical studies of many experimental test results. The Manson-Coffin curves obtained are presented in figure 6.

	σ'_f [MPa]	ε'_f [%]	b	c	K' [MPa]	n'
According to experimental results	702.5	27.2	$-7.82 \cdot 10^{-2}$	$-5.51 \cdot 10^{-1}$	845.3	0.142
UML	812	59	$-8.7 \cdot 10^{-2}$	$-5.8 \cdot 10^{-1}$	893.1	0.15
Medians method	812	45	$-9 \cdot 10^{-2}$	$-5.9 \cdot 10^{-1}$	-	-

Tab. 2: Estimated cyclic properties of the base metal.

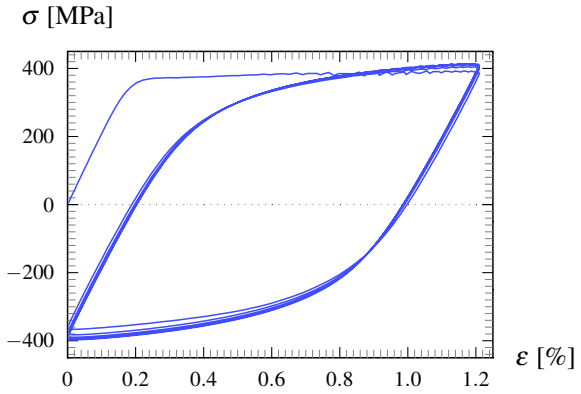

Figure 5: Cyclic tensile curve of the base metal (5 cycles at $\Delta\varepsilon^{t} = 1.209$ %).

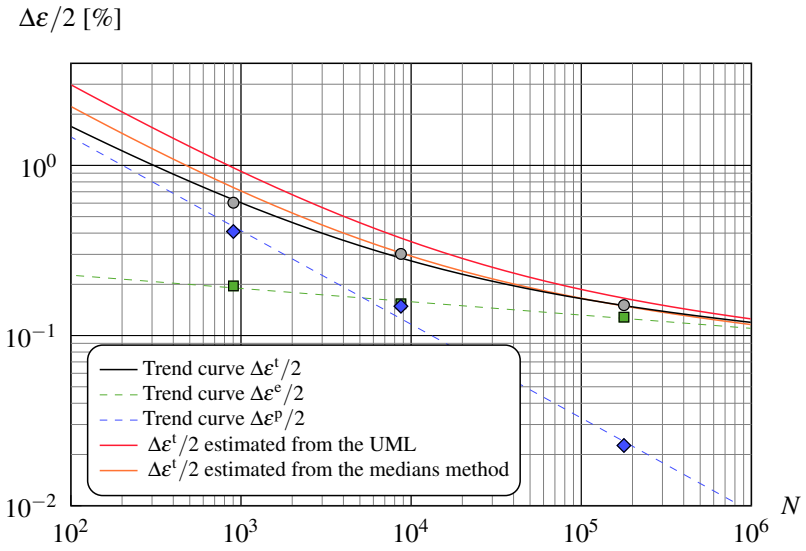

Figure 6: Experimental and estimated Manson-Coffin curves.

3 HFH treatment device

3.1 HFH treatment equipment

The Esonix-type UIT (Ultrasonic Impact Treatment) device was selected to perform high frequency hammer peening treatments (Figure 7). This choice was mainly motivated by the many results given in the literature relating to this hammer model. Comparisons may be made at the end of the treatment.

Figure 7: High frequency hammer peening tool used.

3.1.1 Power supply and excitation frequency

The tool is powered and controlled by an alternating current generator, Esonix PLC05 type. A water cooling device is used to limit transducer heating during the treatment. The generator has 5 power levels which vary the amplitude of the sonotrode vibrations. Whatever is the level of power selected, the excitation frequency remains equal to the resonance frequency of the transducer that is, 27 kHz for the model used.

3.1.2 Indenters

The set of indenters crosses a rubber strip inserted in the removable support in order to keep the indenters in their casing when the tool is inactive (Figure 8).

Indenters with 3 mm in diameter are recommended for the treatment of steel welded assemblies. The detail of their geometry was measured and presented in figure 9. The measurements carried out indicate that the rounded edge has a main radius of approximately 2.4 mm and a secondary blend radius of approximately 0.86 mm. On average, each indenter weights 1.37 g and is 25.6 mm long. The geometry measured will be reused during the numerical simulation of the treatment.

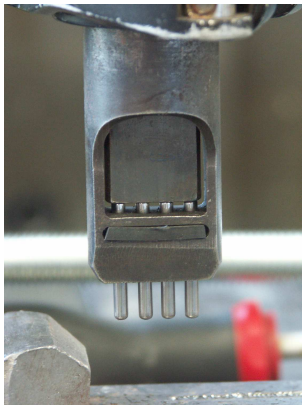

Figure 8: Detail of the indenter support.

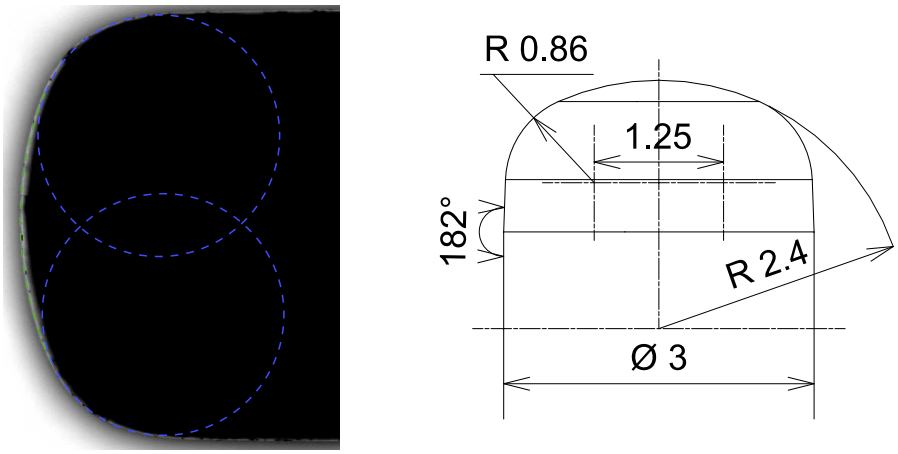

Figure 9: Measured geometry of the 3 mm diameter indenters.

3.1.3 Contact force

The transducer, sonotrode and indenter assembly (hammer peening device) is suspended in the casing in order to isolate the operator from residual vibrations. The suspension spring is pre-stressed upon assembly so that there needs to be a certain pressure for the hammer peening system to be released from stop position during the treatment

Depending on the position of the tool, its weight acts in addition to the pressure applied by the operator. The mean contact force of the indenters on the treated surface was measured for the following three directions:

- In vertical position, indenters directed downwards, the force varies between 60 and 70 N depending on whether the spring is close to the lower or upper stop;
- In horizontal position, it varies between 35 and 45 N, and the weight is no longer involved in the process;
- Finally, in vertical position, indenters directed upwards, the weight acts in opposition and the mean contact force only varies between 10 and 20 N.

3.2 Configuration of the treatment device

A specific assembly was adapted on a conventional milling machine in order to best control the treatment parameters (Figure 10). The tool is assembled vertically above the part to be treated which may be flanged in a sloped position on the moving table. A mobile support guides the hammer in vertical translation with a low stop. Depending on the vertical position of the table, this low stop helps to adjust and constantly maintain the contact force value. In addition to the direction of the tool or the part and the contact force, this assembly helps to simply control the pass speed by taking advantage of the automatic feed system of the milling machine table.

Figure 10: Semi-automatic treatment device.

3.3 Standard parameters and treatment conditions

The high frequency hammer peening treatment tests were carried out in various configurations. Only one parameter varies at a time with the following standard values for the stationary parameters:

- Vertical position, indenters directed downwards;
- Contact force of the indenters of 70 N;
- Feed rate of 400 mm/min;
- One single pass;
- Maximum power level (5/5);
- 23° angle between the tool axis and the normal at the assembly main plate;

- Four 3 mm diameter indenters (or three 4.8 mm diameter indenters) aligned in the treatment direction for the tests on the base metal;
- Reduced to only two 3 mm diameter indenters (or one 4.8 mm diameter indenter) for the welded assemblies.

The number of indenters for the treatment of welded assemblies was decreased due to the difficulties experienced in following the profile of the weld toes. There is greater freedom of movement in the vertical direction obtained using only 2 indenters and no untreated zone was observed.

It is worth noting that the indenters are consumables. The 3 mm diameter indenters were renewed on a regular basis in order to prevent any failure during treatment. Otherwise, if they are used for an extended period this would cause either their strain for low feed rates stemming from a greater heating (causing a blue stain at the end of the indenters through surface oxidation), or fatigue failure in their housing for higher feed rates (refer to figure 11).

Finally, ear protection is recommended in order to attenuate the noise generated by the ultrasonic transducer and by the repeated impacts of the indenters between the sonotrode and the surface of the part to be treated. For information, a 96 dBA sound level was recorded at a distance of 50 cm from the edge of the tool during treatment. This level is higher than that expected based on the literature.

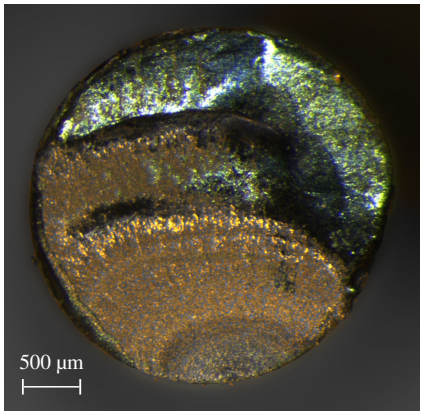

Figure 11: Fracture surface of a 3 mm indenter.

4 Analysing the effects of high frequency hammer peening

4.1 Aspect of the grooves treated

The general aspect of the grooves treated was measured for a set of base metal samples. Figure 12 shows the development of the groove for 3 different treatment power levels. Hammer peening striations appear whatever is the power used. For a greater hammering power, a border is formed at the edge of the hammered zone given by the greater depths of penetration reached (case c). This border expands at a lower treatment speed (case d). Furthermore, in the case of 2 passes at 315 mm/min, damage is created in the hollow of the groove. The one pass treatment at 160 mm/min which corresponds to a theoretical coverage rate closer to case f does not feature this damage, however there is a heightened groove depth. These differences may stem from the fact that the heating has less time to be dissipated at lower treatment speed. Finally, the aspect of the groove obtained with the 4.8 mm diameter indenters is given for example. The kinetic energy transmitted to the indenters is then distributed over a larger contact surface which tends to explain the moderate depth of the groove obtained in this last case.

The operation was then repeated on the cruciform welded assemblies and presented in figure 13. The striations marked by hammer peening can be found on every grooves. The borders are less pronounced even at lower treatment speed. The hardness at the weld toe may explain the limited formation of borders and the moderate depth of the grooves obtained in comparison to the base metal which is softer. It can also be noted that at low power (case a), the initial weld toe is still present in places. Furthermore, a "flaking" type damage appears on occasions and more specifically for cases d and f. A lower coverage rate (case c et e) is therefore to be recommended in order to limit the flaking phenomenon on surface. Finally, it should be noted that the treatment with the 4.8 mm diameter indenters results in a significant improvement of the weld toe radius. However, the treatment depth obtained remains limited in this last case. An excessively closed toe angle may prevent this type of indenters from reaching the weld toe itself.

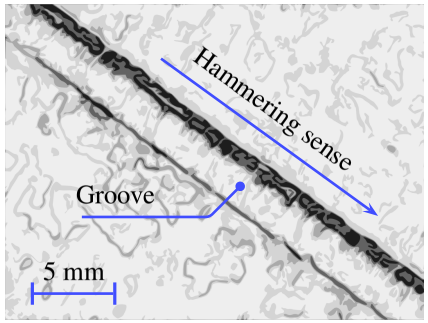

General information

ⓐ Level 1

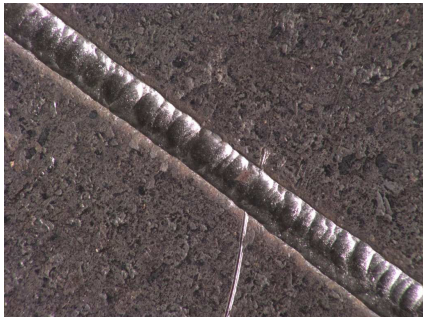

ⓑ Level 3

ⓒ Standard parameters (Level 5)

ⓓ 160 mm/min

ⓔ 630 mm/min

ⓕ 315 mm/min in 2 passes

ⓖ Three 4.8 mm diameter indenters

Figure 12: Change of the hammered groove on the base metal for various treatment parameters.

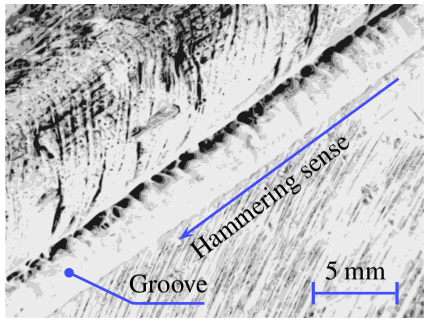

General informations

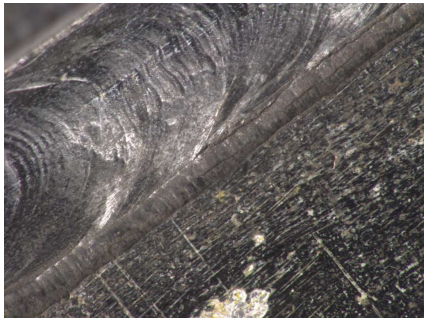

ⓐ Level 1

ⓑ Level 3

ⓒ Standard parameters (Level 5)

ⓓ 160 mm/min

ⓔ 630 mm/min

ⓕ 315 mm/min in 2 passes

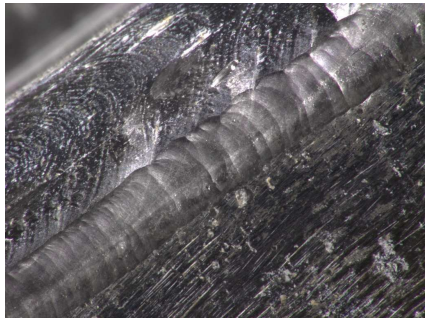

ⓖ One 4.8 mm diameter indenter

Figure 13: Change of the hammered groove on the welded assembly for the various treatment parameters.

4.2 Profiles of the grooves and surface roughness

4.2.1 Measurements by mechanical contact

A first series of measurements was carried out by mechanical contact using a "Somicronic-Surfascan 35" profilometer. These measurements were performed on a length varying from 1.6 to 5 mm based on the accessibility of the probed zone at the rate of one measurement point every 2 µm.

Various profiles measured in the transverse direction to the groove on a welded assembly hammered with the standard parameters are listed in figure 14. Other measurements were carried out in the longitudinal direction of hammer peening on this same sample and recorded in figure 15.

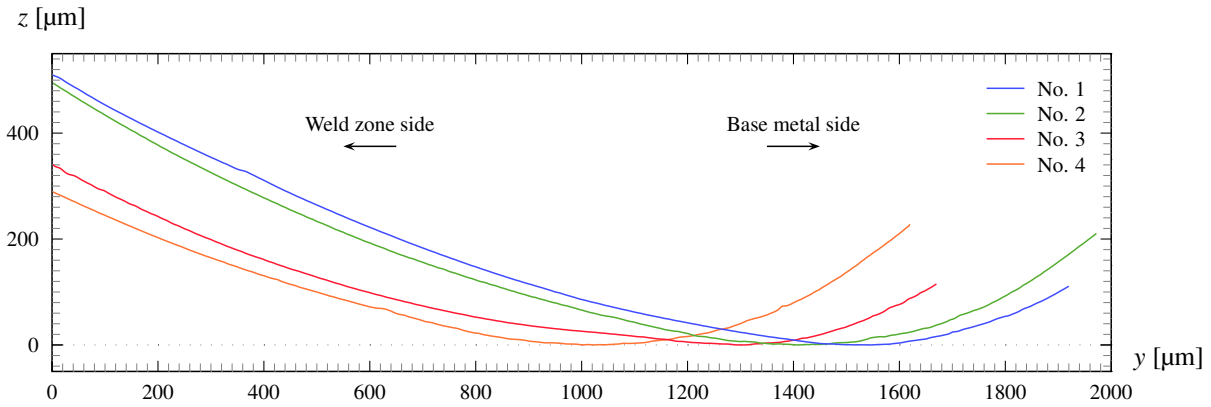

Figure 14: Profiles measured transversally in the groove (case of a welded assembly).

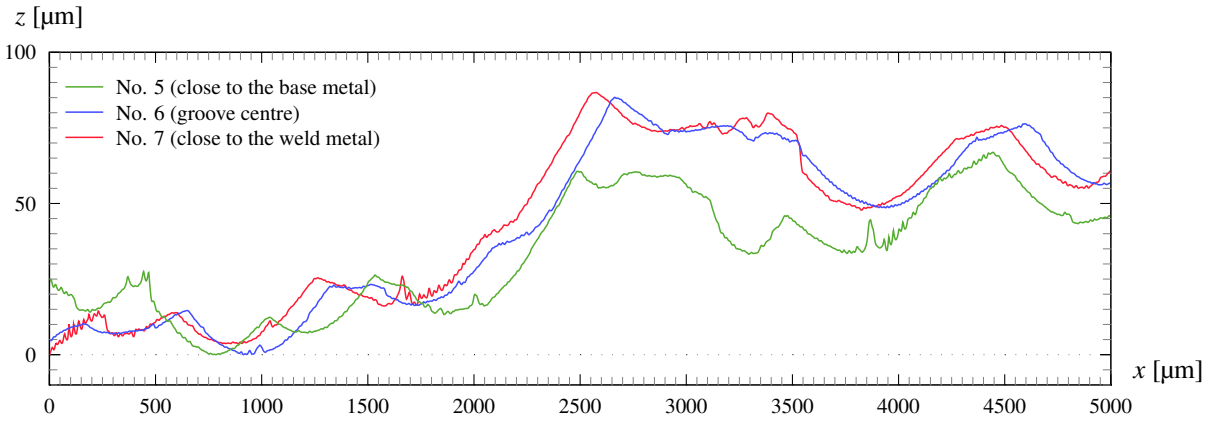

Figure 15: Profiles measured longitudinally in the groove.

The results obtained reveal that there is a certain uniformity for each of the two measurement directions:

- In the hammer peening direction, the shape defects observed correspond to striation separating each of the imprints left by the indenters;
- In the transverse direction, the general profile obtained is much more even. It is very similar to the geometry of the indenters sloping in the base metal direction corresponding to the direction of the tool upon treatment.

From a macroscopic standpoint, it can be noted that the groove radius in the zone with greater stress raiser corresponds more to the blend radius of the indenters than their main tip radius (Figure 9).

On a smaller scale, the roughness deduced from the previous data is given in table 3. Maximum roughness height R_t remains generally less than 4 µm in the transverse direction to the groove and ranges between 10 and 20 µm in the collinear direction. These values associated with the blend radius obtained at the weld toe are especially interesting with respect to the fatigue strength of welded assemblies, given the irregularities usually present in this zone.

	No. 1	No. 2	No. 3	No. 4	No. 5	No. 6	No. 7
R_t [µm]	1.7	1.9	1.6	3.7	18.5	13.7	14.4

Tab. 3: Transverse (1 to 4) and longitudinal (5 to 7) roughness measurements in the groove of a weld toe hammered with the standard parameters.

4.2.2 Optical measurements

- Methodology:

An optical measurement analysis was also carried out using a "Stil-Micromesure 2" station. The optical pen selected enables a lateral precision less than 0.1 µm for a vertical precision of a few nanometres. However, the measurement range is limited to 300 µm in depth and a maximum slope of the scanned surface of +/- 28°. Given that the slope at each edge of the hammered groove is too steep to be detected by the selected optical pen, the measurement zone was limited to the centre of the groove over a width of 2 mm (width of the grove: 3 mm). The measurement spacing was set to 1 µm in both directions.

The three-dimensional surface obtained on a base metal sample (hammered with the standard parameters) is given in figure 16. Impressions 1 to 9 correspond to those of the last of the 4 indenters which contributed to generate the groove.

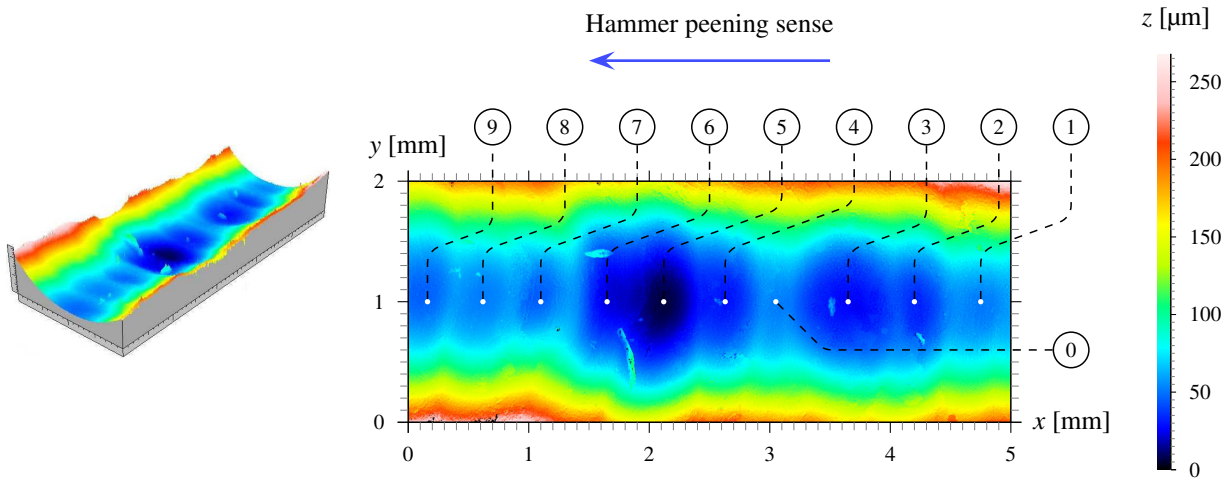

Figure 16: 3D surface and depth level (along z), expressed in false colours of the central zone of a groove from a base metal hammered.

- Estimation of the hammer peening frequency:

Whereas a constant feed rate was dictated at 400 mm/min for this sample, the impacts generated by the treatment device are visibly not quite periodic. The zone of index 0 separating the 3rd and 4th impacts corresponds moreover to a space that was not hammered by the last indenter.

All these impacts make it possible to estimate a mean hammer peening frequency of approximately 48 Hz for the analysed sample by considering:

$$f_{moy} = \frac{N \times v \times n}{l} \tag{1}$$

With: N the number of indenters; n the number of impacts identified; v the feed rate (in m/s); l the analysed length (in m)

In the case of the welded assembly treated with the standard parameters, an optical microscopic analysis helped to identify a set of 49 impacts over an analysed length of 3 cm (that is, a distance between impacts of approximately 60 µm). By applying the relation proposed (1), we obtained a mean hammer peening frequency of 21.8 Hz (for 2

indenters used). This result is similar to that estimated on the base metal from figure 16 if only the frequency per indenter is considered, that is 12 Hz on the base metal and 10.9 Hz on the welded assembly. These hammer peening frequencies are however markedly less than those given in the literature. For example, the frequency measured by Statnikov et al. [2004] range between 200 and 350 Hz for 4 indenters, that is between 50 and 87.5 Hz per indenter.

4.3 Microstructure and surface defects caused

In addition to the peeling (or flaking) observed on surface for high coverage rates, figure 17 reveals the presence of material folds which appear more occasionally and essentially for higher treatment powers (levels 4 and 5). Figure 18 gives an example of the microstructure identified in the treated weld toe. As observed in the literature, the grains are moderately elongated in depth and more pronounced on surface. It should be noted that the depth of the groove caused by the tool for the standard parameters is approximately 0.2 mm.

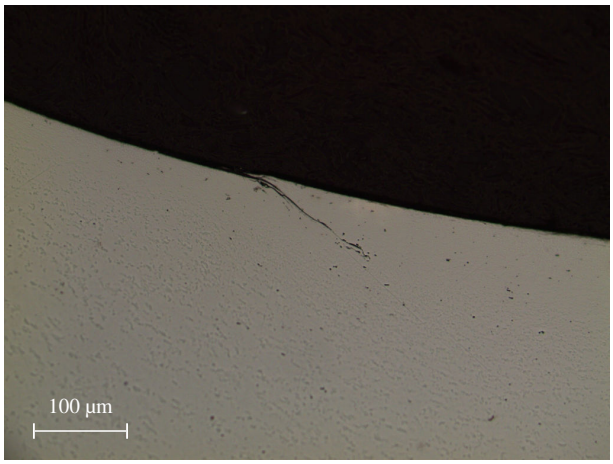

Figure 17: Fold type defects on the base metal sample treated with standard parameters.

4.4 Residual stresses

X-ray diffraction measurements were carried out using a chrome tube and a linear detector (making it possible to register the radiation of the chrome for the family of lattice planes (211) of phase α of the steel), on 3 different specimens:

- Base metal hammered along a line with standard parameters (Figure 19);
- Cruciform welded assemblies treated at the weld toe with standard parameters (Figure 20);
- Cruciform welded assemblies treated then submitted to fatigue loading before the residual stress measurements (Figure 21).

The collimator used leads to an irradiated volume of 2.5 (longitudinally) $\times$ 1.0 (transversally) $\times$ 0.006 (depth) mm^3. The decision was made not to carry out any specific preparation of the groove surface for these measurements except for cleaning with hydrochloric acid. The analyses were carried out along the longitudinal and transverse directions of the groove.

The results, presented in figures 19, 20 and 21, are only qualitative given the non-flat geometry of the groove and its surface roughness (striations) which affects the accuracy of the results. However it can be observed that:

- Relatively high compressive stresses are present on the edge of the groove in both directions;
- The longitudinal stresses in the hollow of the groove are strongly compressed (between -300 and -600 MPa) whereas the transverse stresses are subject to low compression;
- Fatigue loading does not result in significant relaxation of the transverse residual stresses located in the hollow of the groove.

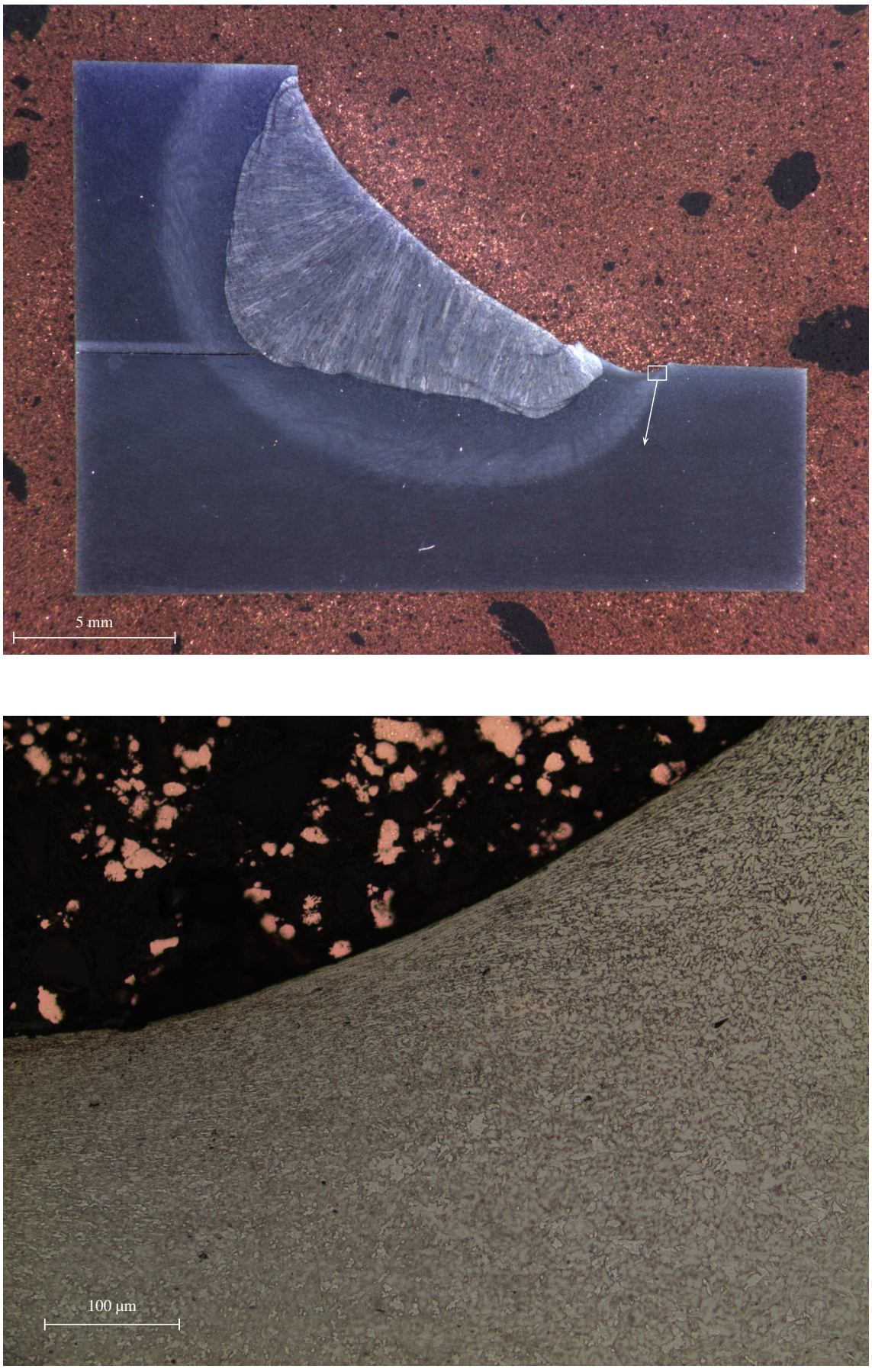

Figure 18: General microstructure of the weld zone treated with standard parameters and magnification at the impacted surface on base metal side.

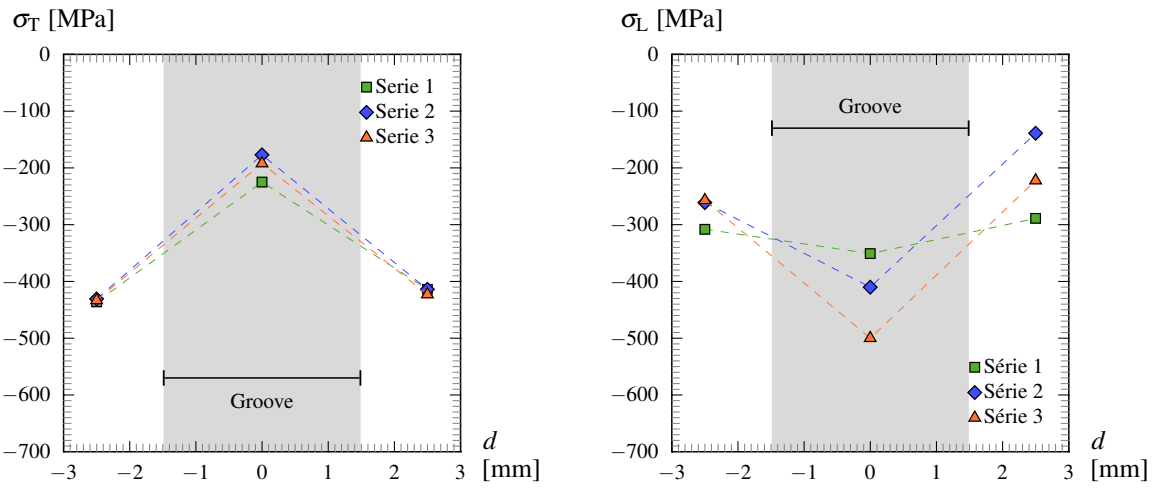

Figure 19: Transverse (left hand side) and longitudinal (right hand side) residual stresses with respect to the groove, measured on a base metal sample hammered with the standard parameters.

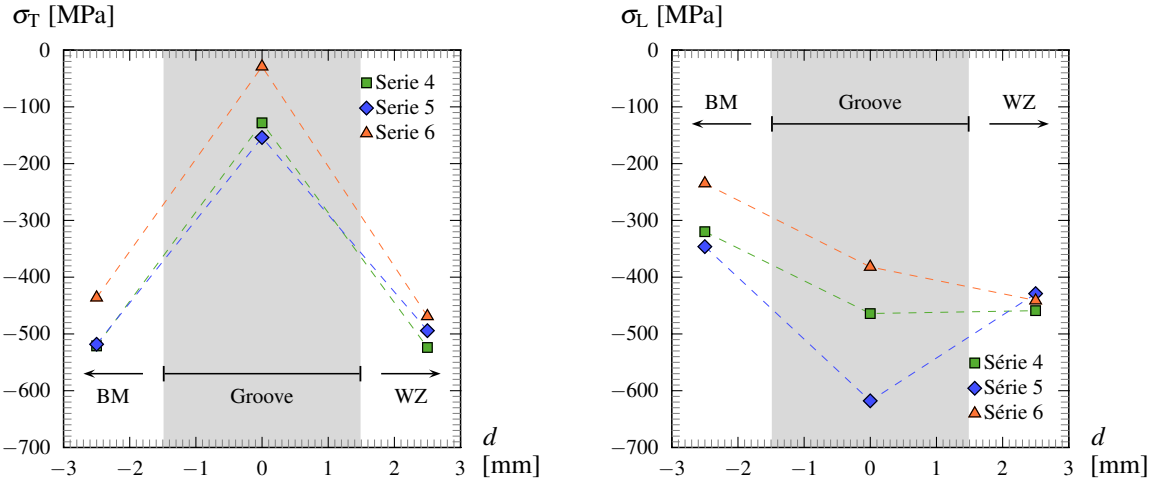

Figure 20: Transverse (left hand side) and longitudinal (right hand side) residual stresses with respect to the groove, measured on a cruciform welded joint hammered with the standard parameters.

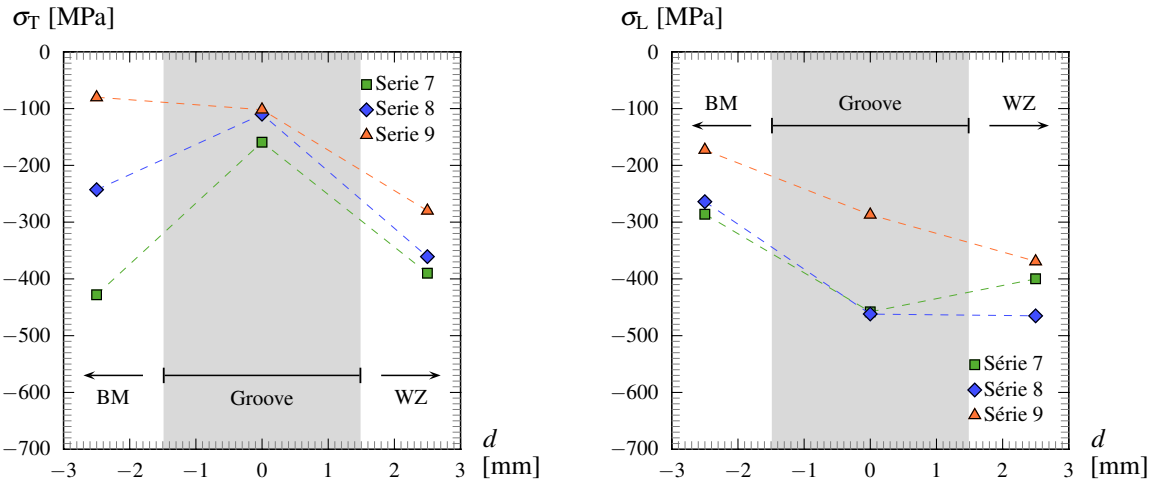

Figure 21: Transverse (left hand side) and longitudinal (right hand side) residual stresses with respect to the groove, measured on a cruciform welded joint hammered with standard parameters and fatigue loaded (95 000 cycles at $R = -1$ and $\Delta\sigma = 566$ MPa).

5 Fatigue tests

5.1 Configuration of the tests specimens

After treatment, the weld test coupons (Figure 1) were cut and machined in order to make the fatigue test specimens. The geometry of the specimens is specified on figure 22.

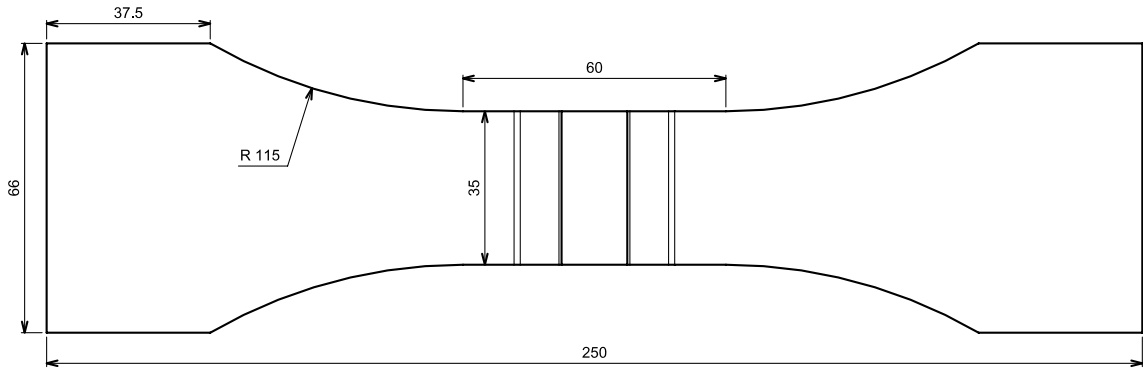

Figure 22: Dimensions of the fatigue specimens (in mm).

5.2 Fatigue test results

Reverse tensile tests ($R = -1$) were carried out on the as-welded cruciform welded assemblies or after hammer peening treatment. Figure 23 highlights the satisfactory fatigue strength of the as-welded assembly, in compliance with the previously mentioned welding quality, as well as the remarkable increase of fatigue life in the case of the treated assemblies, especially for long lives.

On the same figure, the base metal fatigue curve at 50 % of failure probability, estimated by extrapolation of the low cycle fatigue curve, was presented in red doted line. In theory, this curve represents the optimum fatigue strength which may be reached by the treated welded assemblies. As a matter of fact, if treatment gives rise to greater fatigue strength of the hammered zone than that of the base metal, the latter becomes the dimensioning element of the assembly.

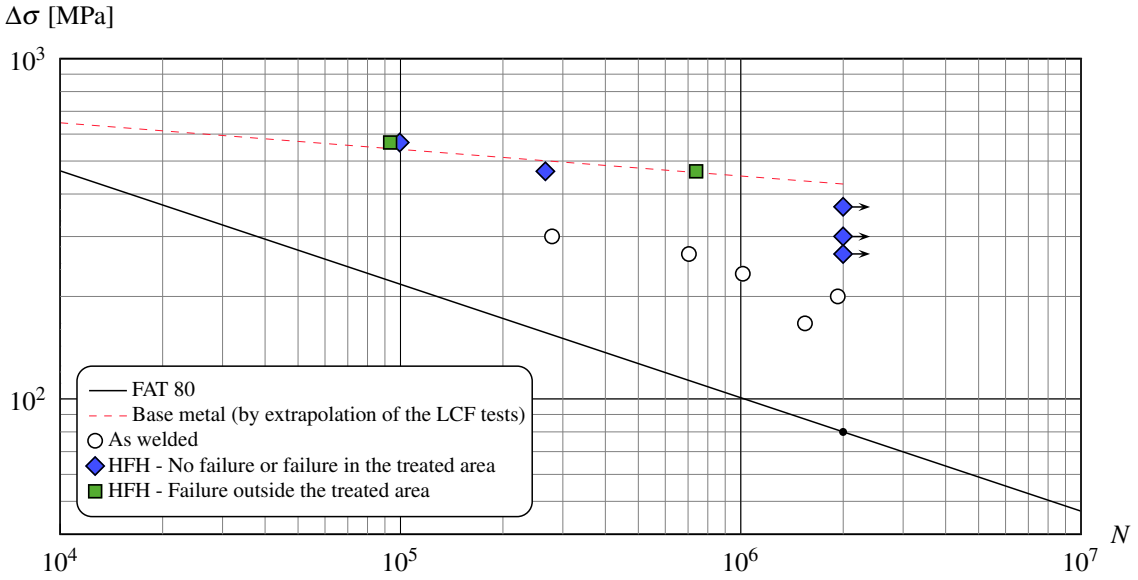

Figure 23: Fatigue results of the welded joints at $R = -1$ and related estimations.

5.3 Fracture surface

The stress ratio $R = -1$ results in a caulking of the crack surfaces which restricts analysis. However on figure 24, several radial lines can be seen around the hammered surface. These radial lines are due to multiple initiations and joining of micro cracks in the hollow of the groove caused by hammer peening.

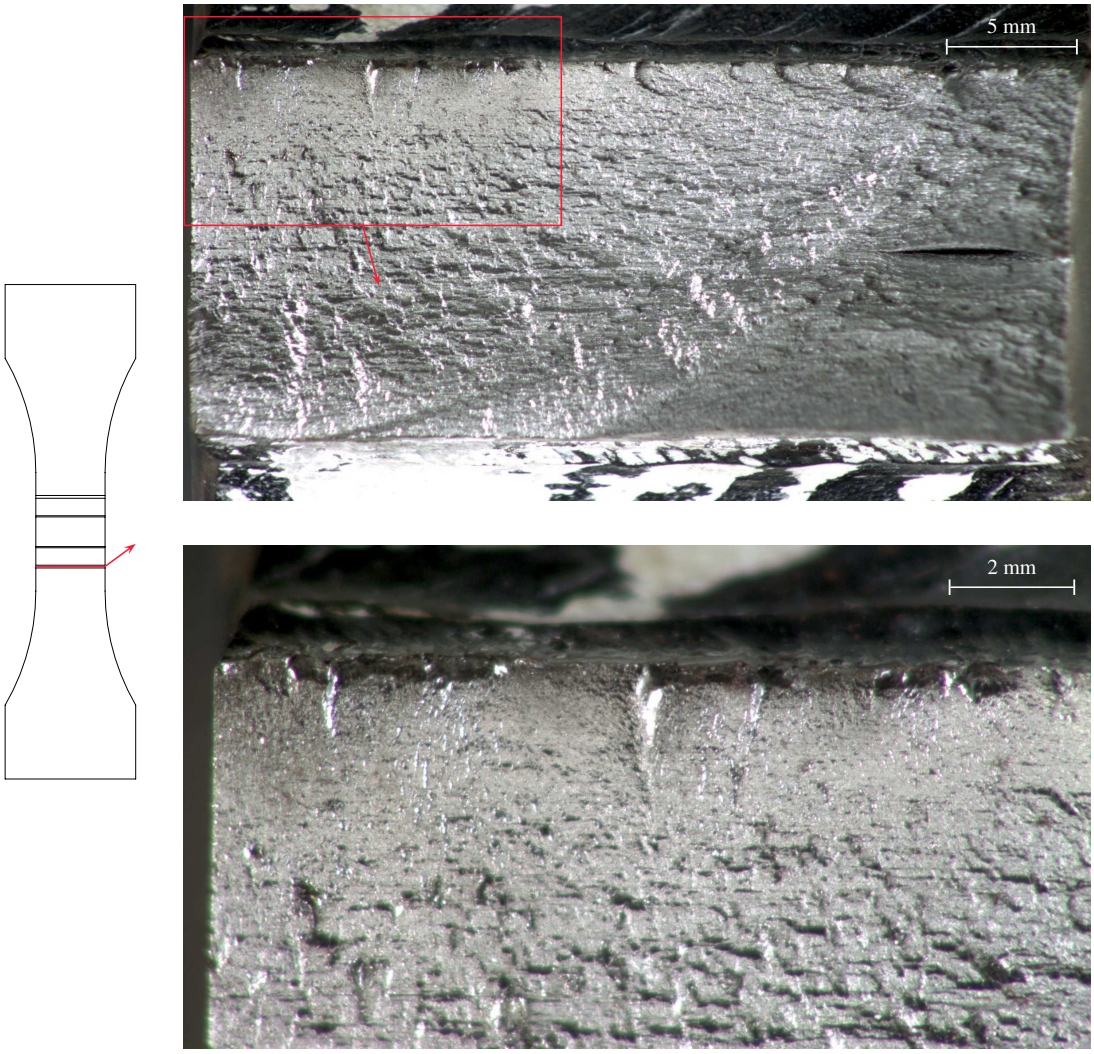

Figure 24: Fracture surface of a welded assembly treated by HFH and broken in the hammered zone.

For the specimens broken outside of the hammered zone, a single initiation point was noted. This initiation point is located on the edge at the end of the calibrated zone (moderate stress raiser location).

6 Results of additional tests

An additional test campaign was carried out on the specimens treated either by manual process or the milling machine by using the same hammer peening device. The treatment was applied in two cases:

- Cruciform welded assemblies composed of DH36 steel (grade for marine application equivalent to S355);
- Butt-welded assemblies composed of S690QL steel.

6.1 DH36 cruciform welded assemblies

It can be noted on figure 25 that the improved fatigue strength of the treated assemblies (blue points) is not significant in comparison to the results obtained on the as-welded assemblies (black triangles). However, a significantly

better gain for the manually treated assemblies can be noted with a tool direction and treatment speed as close as possible to that of treatments on the milling machine.

The slight improvement obtained on these cruciform assemblies can partly be explained by the quality of the weld and the relatively low connecting angle at weld toe.

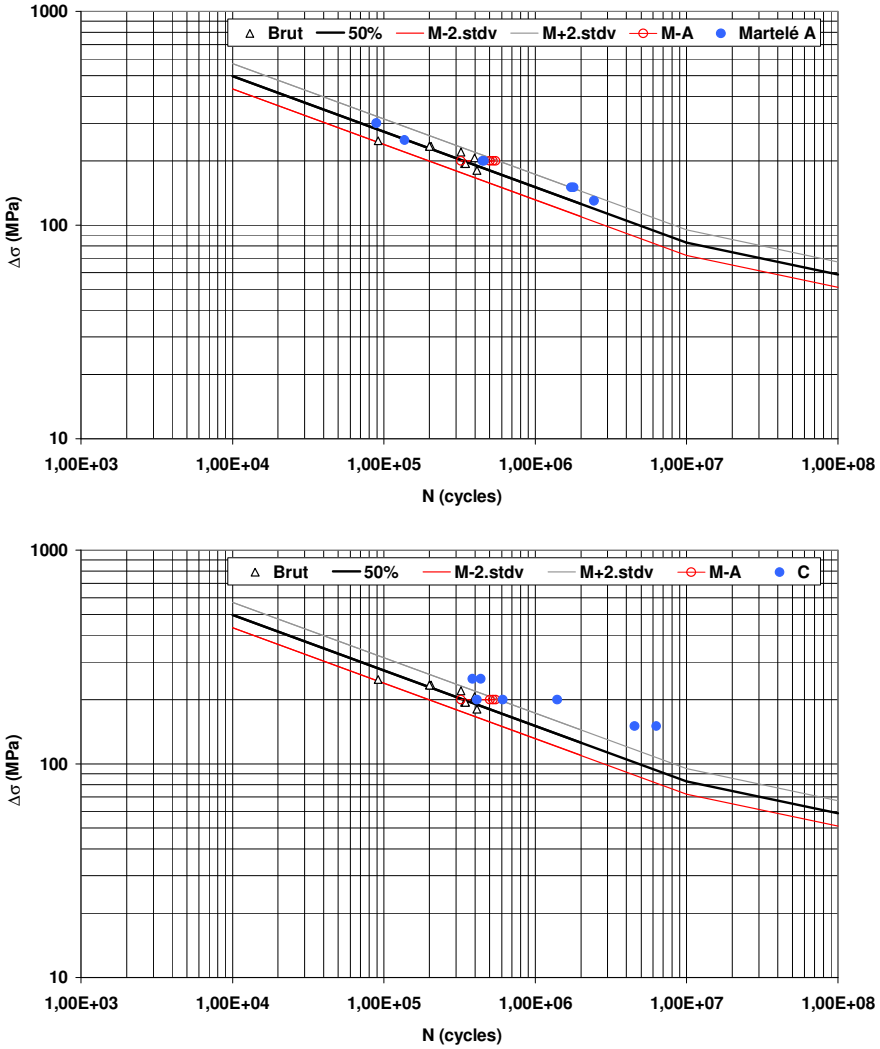

Figure 25: Fatigue results at on cruciform joints composed of DH36 steel for treatment on a milling machine (top) and manually (bottom)[Bousseau, 2010a].

6.2 S690QL butt-welded assemblies

In this case as well, a slight improvement is noted on the treated assemblies (red points and blue triangles on figure 26) compared with the results of the as-welded assembly (black circles). Here, the connecting angle at weld toe and the initial general quality of the welded assembly does not explain the low gain obtained. However, the analysis of the fracture surface highlights a crack initiation located at the bottom of hammer peening folds (Figures27 et 28). Figure 28 in particular reveals a partially propagated crack, initiating once again at a fold at the bottom of the groove.

The formation of a hammer peening fold can be explained through a false direction of the tool at the time of treatment of the butt-welded assemblies. As a matter of fact, in the case in question, the angle of incidence of the indenters was set at 6° with respect to the normal at the assembly sheet. In this direction, the indenters first impact the weld toe from the side of the weld zone and fold a part of the metal under the indenter itself, in the stress raiser zone, creating the folds observed.

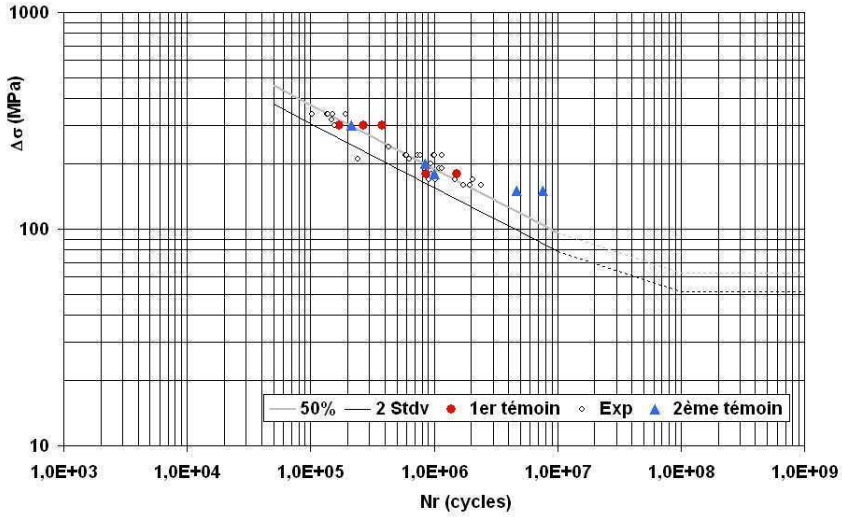

Figure 26: Fatigue results at $R = 0.1$ on butt-welded joints composed of S690QL for treatment on a milling machine [Bousseau, 2010b].

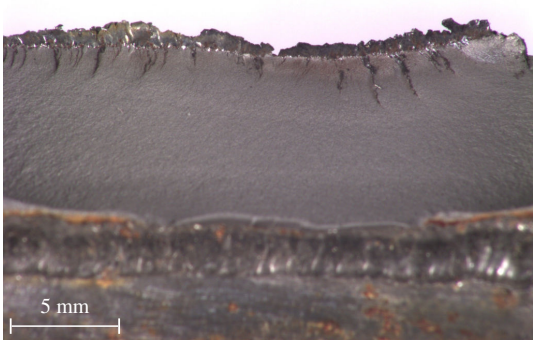

Figure 27: Fracture surface of a S690QL butt-welded assembly.

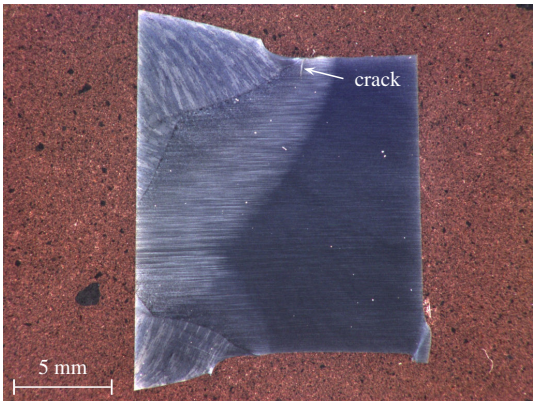

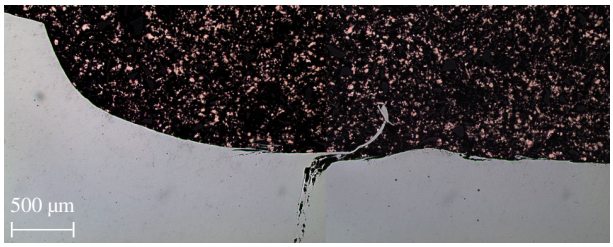

Figure 28: Microstructure of a S690QL butt-welded assembly treated by HFH and detail of the crack initiation zone at the bottom of the groove.

7 Conclusions

The aim of this study was to better understand the effect of HFH parameters on the fatigue life improvement provided of steel welded assemblies. The following points are worthy to be noted:

- With optimized hammer peening treatment conditions, the results obtained are well in line with those of the literature;
- Even though the welded assemblies have good behaviour in the as-welded state, a significant improvement in fatigue strength was noted after treatment;
- The residual compressive stresses measured in the groove created by HFH are relatively low in the loading direction;
- The improvement of the local geometry and moving the initiation point with respect to the initial weld toe are significant parameters;
- The reduced number of indenters (2 instead of 4 normally used) does not seem to have affected these results;
- The estimated hammer peening frequency is markedly lower than those indicated in literature;
- The results presented on several assembly batches seem to highlight the importance, on the one hand, of the initial weld toe geometry and, on the other hand, the conditions of use of the tool (direction, pressure, etc.) in relation to the risk of hammer peening folds appearing.

This study therefore reveals the importance of developing a consistent and robust approach with the aim of defining the optimum operating conditions of the process.

References

M. Bousseau. Parachèvement par le procédé UIT d'un joint soudé en croix en acier DH36. Technical Report C-09196 Ind. A, DCNS (CESMAN), 2010a. (Page 18)

M. Bousseau. Parachèvement par le procédé UIT de joints soudés bout à bout en acier S690QL. Technical Report C-09232 Ind. A, DCNS (CESMAN), 2010b. (Page 19)

A. J. Bäumel and T. Seeger. *Materials Data for Cyclic Loading - Supplement I.* Elsevier Science, 1990. (Page 4)

G. Le Quilliec, M. Drissi-Habti, G. Inglebert, H.-P. Lieurade, and P. Macquet. Traitement des assemblages soudés par martelage haute fréquence. *Revue des Composites et des Matériaux Avancés*, 19(1):73–101, 2009. (Page 1)

M. A. Meggiolaro and J. T. P. Castro. Statistical evaluation of strain-life fatigue crack initiation predictions. *International Journal of Fatigue*, 26:463–476, 2004. (Page 4)

NF EN 10025-2. Produits laminés à chaud en aciers de construction, 03 2005. (Pages 2 and 4)

E. S. Statnikov, V. Vityazev, and O. Korolkov. Comparison of the efficiency of 27, 36 and 44 kHz UIT tools. *International Institute of Welding (IIW)*, (XIII-2005-04), 2004. (Page 13)